INTERNATIONAL JOURNAL OF CLIMATOLOGY
Int. J. Climatol. **32**: 831–842 (2012)
Published online 7 April 2011 in Wiley Online Library
(wileyonlinelibrary.com) DOI: 10.1002/joc.2310

RMetS
Royal Meteorological Society

ENSO-conditioned rainfall drought frequency analysis in northwest Baja California, Mexico

M. Hallack-Alegria,[a] J. Ramirez-Hernandez[b]* and D. W. Watkins, Jr.[c]

[a] *Titular Professor, Engineering and Technology Center, Universidad Autonoma de Baja California, Mexico*
[b] *Titular Researcher, Engineering Institute, Universidad Autonoma de Baja California, Mexicali, Baja California, México*
[c] *Associate Professor, Department of Civil and Environmental Engineering, Michigan Technological University, Houghton, Michigan, USA*

ABSTRACT: Located in northwest Baja California, Mexico, the Guadalupe River Basin is situated in a semiarid region where periods of drought pose serious economic, social and environmental concerns. The study area has highly variable climate, with mean annual precipitation ranging from less than 12 mm to over 750 mm a year across the basin, and with most of the annual precipitation occurring during the autumn and winter seasons. To quantify the frequency and severity of meteorological droughts at the local (watershed) scale, this study investigates seasonal and annual precipitation data from 34 sites in northwest Baja California. Along with the analysis of precipitation climatology and interannual variability, El Niño/Southern Oscillation (ENSO) and related Pacific Ocean sea surface temperature (SST) patterns are shown to be potential predictors of seasonal precipitation. Analysis of precipitation variability at seasonal and annual time scales is performed using the standardized precipitation index (SPI) methodology, and annual, seasonal, and ENSO-conditioned precipitation frequency analyses are executed using the regional L-moment algorithm. The SPI and regional rainfall drought frequency estimates developed in this study may be useful for monitoring meteorological droughts and could serve as critical components of a comprehensive drought management plan. Furthermore, the methods applied in this study may be transferred to other semi-arid locations to mitigate drought risk and, potentially, impacts of drier conditions in the 21st century. Copyright © 2011 Royal Meteorological Society

KEY WORDS drought; Mexico; L-moments; standardized precipitation index; multivariate ENSO index; El Niño/Southern Oscillation

Received 19 December 2009; Revised 17 January 2011; Accepted 23 January 2011

1. Introduction

The water resources of Mexico are generally abundant, with precipitation over the country totalling approximately 1511 cubic kilometers of water per year. However, about 72% of this rainfall evaporates, and half the precipitation is concentrated in the southern portion, which represents only 20% of the total area. In contrast, only 25% of this precipitation occurs in the northern portion of the country that represents 50% of the total area (CNA 2004). Hydroclimatic variability is of particular interest if we consider that the population of Mexico has quadrupled in the last 55 years, and in general, greater population and economic growth has occurred in the zones with less water availability. Thus, 77% of the population is now concentrated in the central and northern parts of the country that account for only 31% of the national water availability. Accordingly, in only 55 years, Mexico has moved from an average availability of 18,035 m^3/yr/person to 4,416 m^3/yr/person, which positions the country in a situation of water stress (CONAGUA 2007).

Additional concern arises from evidence that North America is in transition to a more arid climate as part of a general drying trend and poleward expansion of the subtropical dry zones (Held and Soden 2006; Lu *et al*., 2007). Moreover, there may be a strengthening north-south pattern in drought trends (Dai *et al*., 2004), explained by precipitation decreases that have occurred mainly in southern and western Canada, Alaska, and Mexico (Kunkel *et al*., 2008). North American droughts fit into a global pattern of hydroclimatic variations (Seager 2007). For example, persistent below-normal precipitation during 1998–2002 led to regional droughts stretching from western North America to the Mediterranean, southern Europe, and even southwest and central Asia (Hoerling and Kumar 2003). Further complicating water resources planning, climate extremes show significant spatial variability, and in North America it is not unusual for severe drought and flooding to occur at the same time in different locations (Kunkel *et al*., 2008).

This study focuses in the Guadalupe River Basin located in northwestern Baja California (Figure 1), where water is used for agricultural irrigation and also to supply a nearby city. The basin has an area of about 2380 km^2, with agriculture, primarily grapes and olives, the predominant land use. The region is semi-arid, and

* Correspondence to: J. Ramirez-Hernandez, Titular Researcher, Engineering Institute, Universidad Autonoma de Baja California, Mexicali, Baja California, México. E-mail: jorger@uabc.edu.mx

Figure 1. Location of the Guadalupe River Basin and the precipitation stations used in this study. This figure is available in colour online at wileyonlinelibrary.com/journal/joc

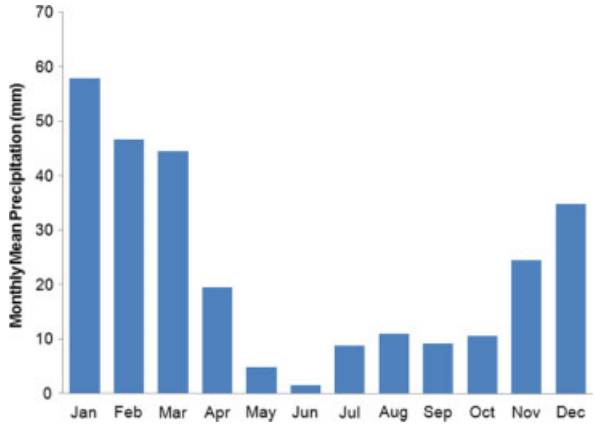

Figure 2. Monthly mean precipitation for the period 1950–2008 for the area corresponding to the Guadalupe River Basin. This figure is available in colour online at wileyonlinelibrary.com/journal/joc

the average monthly rainfall distribution of the study area (Figure 2) indicates a typical Mediterranean climate, with greater rainfall in autumn and winter months (Gaeta-Lara 2006). It is during this time of year that the semi-permanent North Pacific anticyclone weakens, allowing the entrance of convective and frontal systems into the region (Arriaga-Ramirez and Cavazos 2010). Due to interannual variability in cyclone and anticyclone activity, there is high interannual variability in precipitation (CNA 2006), and persistent droughts are a reality that greatly affects agricultural activity and water supply in the region (Waller-Barrera 2008). Furthermore, rapid population and economic growth is occurring in the basin. According to estimations made by the local water utility, water demand was met in a sustainable way only until 2006, forcing a search for alternative water sources to the Guadalupe River Basin and surrounding towns (Medellin-Azuara *et al*., 2007). In semi-arid regions such as this, with rapid economic and population growth, as well as flourishing agricultural activity, water resources planning is critical to long-term economic and environmental sustainability (Hallack-Alegria 2005). Consequently, there is an increasing need to understand the occurrence and predictability of drought in the region and mitigate events that may cause severe damage (Block and Rajagopalan, 2007).

Along these lines, much effort has been made to develop seasonal to annual hydroclimatic forecasts for water management in different parts of the world (e.g. Gershunov and Cayan 2003; Wei and Watkins 2011). Studies in northwest Mexico and southwest USA have found rainfall is influenced by strong interannual variability of atmospheric circulation, much of which is associated with the El Niño/Southern Oscillation (ENSO) (e.g. Schonher and Nicholson 1989; Cayan *et al*., 1999; Higgins *et al*., 2007). Similarly, multiyear droughts over southwestern North America have been forced by persistent anomalous sea surface temperatures (SSTs), with cold, La Niña-like, SSTs in the Pacific playing the dominant role (Seager 2007; Cook *et al*., 2007), In northern Mexico ideal drought conditions occur during La Niña and a warm subtropical North Atlantic (Seager *et al*., 2009). Wang *et al*. (2007) showed through composite analyses that during La Niña events, a continental-scale high-pressure anomaly dominates over most of North America and leads to summer drought over the central USA. As found by Hoerling (1997, 2001), during winter the La Niña pattern shifts westward with the high SSTs, thus strengthening the North Pacific anticyclone. The eastern side of the subtropical high, typically centered around a latitude of 30 °N, is associated with subsiding stable air, which produces low relative humidities and dry conditions in Southern California and Northwest Baja California.

From 1950 until the mid-1970s, corresponding to a cool phase of the Pacific Decadal Oscillation (Trenberth and Hurrell 1994), northwest Baja California experienced a moderately dry period (Reyes and Troncoso 2004), but after 1980, two El Niño episodes (1983 and 1998) were responsible for the wettest years on record (Cavazos and Rivas 2004). Reyes-Coca and Troncoso-Gaytan (2001) investigated ENSO impacts on winter precipitation for the 1997–1998 El Niño-event, recreating possible rainfall scenarios and encouraging investigation of rainfall forecasting based on ENSO. Minnich *et al*. (2000) evaluated precipitation variability for the winter season in

Baja California in relation to ENSO using the Southern Oscillation Index (SOI), finding strong correlations between SOI interannual variability and both monthly and annual precipitation. Cayan *et al*. (1998) found that ENSO explains 30% of rainfall interannual variability in the region. Similarly, Cavazos and Rivas (2004) found that ENSO explains 36% of 1-day heavy precipitation variance. Arriaga-Ramirez and Cavazos (2010) investigated regional trends in a range of annual and seasonal daily precipitation indices, finding a statistically significant trend in the frequency of intense winter rainfall events and a significant correlation with antecedent (summer) ENSO activity.

The aim of this paper is to characterize seasonal to interannual meteorological droughts in northwestern Baja California and investigate their modulation by ENSO. Specifically, the research questions addressed are as follows:

- What are the intensity-duration-frequency characteristics of local-scale meteorological droughts in northwestern Baja California, a region with a Mediterranean climate but prone to high rainfall variability and persistent dry periods?
- Does the ENSO phenomena influence meteorological drought in the region, and if so, what are the implications for forecasting drought risk on seasonal time scales?

Previous studies have tended to focus on the link between ENSO and flooding and/or intense rainfall (e.g. Gershunov and Cayan 2003; Cavazos and Rivas (2004), or on the frequency of daily rainfall events and dry spell length (e.g. Higgins *et al*., 2007; Groisman and Knight 2008; Arriaga-Ramirez and Cavazos 2010), without addressing seasonal and annual rainfall totals during dry periods, which may be more relevant for water supply management. Another contribution of this study is that the drought analysis is relevant to local scales, as it is conducted using gage (point) rainfall data rather than output from dynamical models, which must be downscaled to local or watershed scales. Several authors (e.g. Easterling *et al*., 2000; Zhu and Lettenmaier 2007; Higgins *et al*., 2007) have noted that demonstrating ENSO's effect on rainfall variability in the region has been hampered by a lack of accurate and complete long-term precipitation records, a limitation that is partially overcome in this study through a regional frequency approach (e.g. Fowler and Kilsby, 2003; Trefry *et al*., 2005, Wallis *et al*., 2007).

This paper begins with a description of the datasets utilized, followed by an analysis of northwest Baja California climatology and interannual precipitation variability. ENSO and related Pacific Ocean SST patterns are investigated as potential predictors of seasonal precipitation. Analysis of local meteorological droughts at seasonal and annual time scales is performed using the standardized precipitation index (SPI) methodology. Finally, regional seasonal, annual and ENSO-conditioned precipitation frequency analyses are executed based on a regional L-moments algorithm (Hosking and Wallis, 1997) to estimate precipitation quantiles at a local (point) scale.

2. Data and analysis methods

The definition and identification of droughts has been the subject of a wide range of studies (e.g. Labedzki 2007). In order to analyse droughts from a statistical point of view it is necessary to specify the subsequent features: the climatic variable that will be used for defining droughts; the characterisation of the spatial and temporal distribution of the defining variable; the truncation levels for classifying drought severity at a specific point; and the quantification of the regional drought (Shin and Salas 2000). Herein, the climatic variable is precipitation, and the focus is solely on meteorological droughts, which are usually expressed in terms of drought indices and can be defined by the degree of dryness and the duration of the dry period (McKee *et al*., 1993, Paulo *et al*., 2005, Labedzki 2007, Hallack-Alegria and Watkins 2007).

A regional frequency analysis approach based on L-Moments (Hosking and Wallis 1997) is performed to produce return period precipitation estimates that have significantly increased reliability over at-site estimates (Wallis *et al*., 2007). The regional frequency analysis methodology used consists of four basic steps: screening of the data, identification of homogeneous regions, choice of a frequency distribution, and estimation of the frequency distribution. In this study, regional precipitation analysis was conducted for the complete dataset using the L-Moment Regional Analysis Program provided by MGS Engineering Consultants (http://www.mgsengr.com/, 2009).

2.1. Data

This study uses data from the period of 1950–2008 because monthly data are not commonly available with sufficient coverage and length of record for earlier periods. The chosen stations are considered to be the best long-term records available. Screening and quality control of monthly precipitation data were needed to remove erroneous values due to transcription mistakes and deficient reporting in various years. The observational monthly precipitation data was compiled from the ERIC III database provided by the Mexican Institute of Water Technology (IMTA) for the period of 1950–2004. Additional data were acquired from the National Commission of Water (CONAGUA) in the state of Baja California for the period of 2004–2008, and to fill in missing data for some stations that coincide in both databases for the 1950–2004 period. Selection of these stations was based on the following characteristics: geographic location, period of record, and precipitation patterns such as mean annual precipitation range and seasonality. Additionally, precipitation data included in the analysis satisfied the following criteria: a minimum of 15 years of

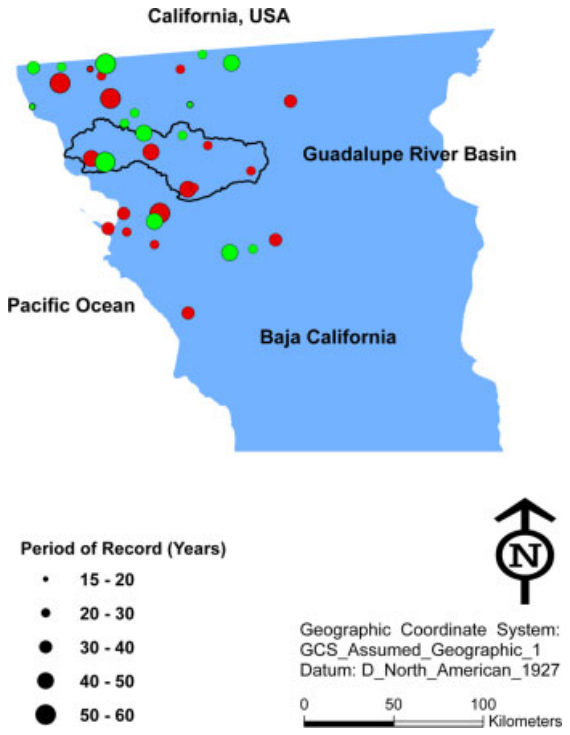

Figure 3. Period of record in years for each station. Green (light) circles represent truncated time series. Red (dark) circles represent continuous time series. This figure is available in colour online at wileyonlinelibrary.com/journal/joc

record at the site and spatial consistency with surrounding gages. However, not all stations had continuous datasets for the period of record, leading to the inclusion of some truncated time series (Figure 3). Out of 55 stations initially selected, a total of 34 met these conditions, with record lengths ranging from 15 to 59 years.

Hosking (1990) asserted that asymptotic biases of L-moment ratios are negligible only for sample sizes of 20 or more, but imposing this requirement in this study would have reduced the number of stations from 34 to 28. The regional L-moment algorithm of Hosking and Wallis (1993) applied herein allows for greater variability of L-moment ratios in small samples (e.g. Guttman, 1994) by weighting the site-specific ratios proportionally to the sites' record lengths. Thus, in this study, the gages with short record lengths are given smaller weight in the regional parameter estimates than gages with longer records, reducing potential bias in the regional quantile estimates.

For the ENSO analysis, events that were listed by the Western Region Climate Center and the NOAA Climate Prediction Center are included in the analysis. The Multivariate ENSO Index (MEI, Wolter and Timlin, 1993) was selected to quantify the magnitude of ENSO. The MEI represents the principal six variables of the observed analysis components in the tropical Pacific: sea-level pressure, north-south component of surface wind, east-west component of surface wind, sea surface temperature, surface air temperature and total cloudiness fraction of the sky (Wolter and Timlin 1993). MEI values were obtained from the Climate Prediction Center website (http://www.cdc.noaa.gov/people/klaus.wolter/MEI/). Positive values represent El Niño, while negative values correspond to La Niña episodes.

Sea surface temperature (SST) fields are also used to analyse correlations with seasonal precipitation. The data used was the extended reconstructed sea surface temperature (ERSST) analysis (Smith *et al.*, 2008), obtained from the National Climatic Data Center (NCDC) through the KNMI Climate Explorer, an online data analysis tool (Oldenborgh and Burgers, 2005).

2.2. Precipitation regions

A homogenous region is formed by sites that can be pooled to improve the reliability of the magnitude-frequency estimates for all stations (Wallis *et al.*, 2007). The arrangement of precipitation regions was made by identifying clusters using the Hosking and Wallis (1997) discordancy criteria to categorize sites whose sample statistics were relatively unusual from the region as a whole.

Since the number of sites in the regions may vary, and the dataset is relatively small (34 stations in total), the critical discordancy values recommended by Hosking and Wallis (1997) (Table I) were followed to identify any sites with discordancy values greater than 2.87 as suspicious. Data for these sites were checked, and any values that were obviously erroneous were manually removed from the site's record. Average annual and seasonal precipitation data for each region were also confirmed to be serially independent and stationary (Wallis *et al.*, 2007).

In order to confirm the identification of homogeneous regions, heterogeneity measures, H1 and H2, were computed comparing the between-site dispersion in sample L-moments for the group of sites with what would be expected from a large sample obtained from a homogeneous region (Hosking and Wallis 1997). H1 is the standard deviation, weighted according to the record length of the at-site L-CV; and H2 refers to the average distance from site coordinates to the regional average on a plot of L-moment ratios, L-CV *versus* L-Skewness (Hosking and

Table I. Critical values for the discordancy measure (Hosking and Wallis 1997).

Number of sites in region	Critical value
5	1.333
6	1.648
7	1.917
8	2.140
9	2.329
10	2.491
11	2.632
12	2.757
13	2.869
14	2.971
≥15	3.000

Wallis, 1997). H1 and H2 measure statistical heterogeneity from known distributions and do not consider any variability that arises from other sources (Wallis *et al*., 2007).

Since L-CV is a critical variable for the formation of regions, H1 is considered to be more important than H2 because variation in the L-CV has a greater effect than variation in the L-Skewness or L-Kurtosis on the precision of the extreme quantile estimates. Hosking and Wallis (1997) suggest regarding a region as acceptably homogeneous if heterogeneity measures, H1 and H2, are less than 1.

2.3. Interannual rainfall variability

The SPI is focused exclusively on precipitation for user-selected (i.e. 3, 6, 12, 24 months) periods of time to assess precipitation accumulations and deficits in a manner that allows for direct (standardized) comparison among different climate regions (McPhee *et al*., 2004). Using calendar years, the SPI was calculated for both regions for each month for the period of record, 1950–2008, for 6, 12, and 24-month time scales, fitting a Gamma distribution as suggested by Wu *et al*., 2005. For this study, SPI values were computed using the software from the National Drought Mitigation Center (http://drought.unl.edu/). The 6-month SPI time scale may be used for seasonal drought identification, the 12-month SPI time scale for intermediate-term drought, and the 24-month SPI for long-term drought (Labedzki, 2007). Positive SPI values indicate wet conditions, while negative values indicate dry conditions.

2.4. Frequency distributions

Following the identification of homogeneous regions, the next task in regional frequency analysis is identifying an appropriate probability distribution for describing the data (Wallis *et al*., 2007). Five three-parameter probabilistic distributions were considered in this analysis: Generalized Normal (GNO), Generalized Extreme Value (GEV), Pearson Type III (PE3), Generalized Logistic (GLO), and Generalized Pareto (GPA). Two-parameter distributions were not considered in this study for the reason that tail quantiles may be seriously biased if the shape of the tail of the true distribution is not well estimated by the fitted distribution (Hosking and Wallis, 1997).

Following the Hosking and Wallis (1997) methodology, a goodness of fit statistic, Z, is the criterion used to select a distribution:

$$Z^{DIST} = (\tau_4^{DIST} - t_4^R + B_4)/\sigma_4$$

where t_4^{DIST} is the theoretical L-kurtosis for a given distribution, t_4^R is the regional average L-kurtosis, B_4 is the correction for the bias associated with t_4^R, and σ_4 is the estimated standard deviation of t_4^R obtained by repeated simulation of a homogeneous region whose sites have record lengths the same as those of the observed data. The procedure indicates 'acceptable' distributions for $|Z| \leq 1.64$, which corresponds to the failure to reject the hypothesized distribution at a confidence level of 90% (Hosking and Wallis 1997).

2.5. Parameter and quantile estimates

The next steps are estimation of parameters and quantiles for each of the acceptable probability distributions for each region. Implicit in the definition of a homogeneous region is the condition that all sites in a region can be described by one probability distribution having common distribution parameters after the site data from each gage are scaled by an index, typically the at-site mean (Wallis *et al*., 2007). Sample L-moment ratios for each site are weighted according to record length and combined to give regional average L-moment ratios, which are use to estimate regional distribution parameters and quantiles (Hosking and Wallis, 1997). Thus, the quantile estimate at site i for the regional $T-$ year event is given by the following equation:

$$\hat{Q}_i(T) = \lambda_1^{(i)} \hat{q}(T)$$

where $\hat{q}(T)$ is the regional quantile estimate and $\lambda_1^{(i)}$ is the site-specific scaling factor, defined as the at-site mean. To smooth sampling variability and to obtain precipitation frequency estimates for any location within the region, the at-site mean values may be smoothed or spatially interpolated using geostatistical methods as described by Watkins *et al*. (2005) or Wallis *et al*. (2007).

3. Results and discussion

3.1. Homogeneous regions

Heterogeneity measures (H1 and H2) indicated that all sites in the study could be considered to lie within a single region, consistent with the precipitation region proposed by Arriaga-Ramirez and Cavazos (2010) in northwest Baja California. However, in this study the discordancy measure was high for several sites, indicating they should be removed from the dataset. To avoid this, it was decided to define two regions physically consistent with the coastal and mountain zones, which reduced the total number of discordant sites. Region 1 contains 21 stations, and Region 2 includes 13 stations (Figure 4). Two discordant sites were found in Region 1, and one discordant site in Region 2. However, applying the heterogeneity tests (Hosking and Wallis, 1997, Wallis *et al*., 2007), both regions were found to be acceptably homogeneous with H1 and H2 <1 (Table II). Furthermore, there was no evidence of gross errors in data from those three sites, so they were kept in the analysis.

3.2. Seasonal and interannual variability

Figure 4 depicts the spatial variability of precipitation in the study area, where the annual average precipitation is 280 mm and the lowest precipitation totals are in the coastal zone, Region 1. Temporal variability may

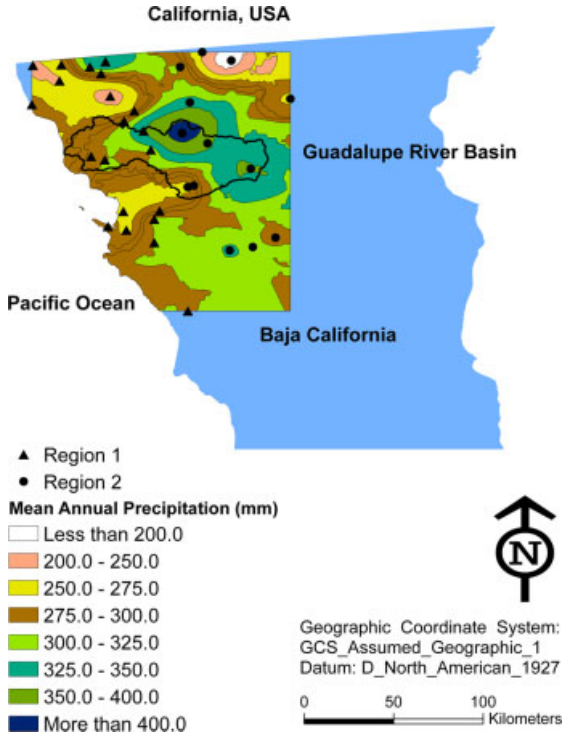

Figure 4. Proposed precipitation regions and mean annual precipitation for the study area. Precipitation map developed using the geostatistical method of kriging (e.g. Chapman and Thornes, 2003) provided by the ArcMap GIS software (ESRI ArcMap 1999–2006, http://www.esri.com). This figure is available in colour online at wileyonlinelibrary.com/journal/joc

Table II. Results of heterogeneity test for Regions 1 and 2.

	Heterogeneity measure	
	H1	H2
Region 1	0.48	−2.58
Region 2	−1.94	−1.77

Table III. Classification of SPI values (McKee *et al.* 1993).

SPI values	Category
>2.00	Extremely wet
1.50 to 1.99	Very wet
1.00 to 1.49	Moderately wet
−0.99 to 0.99	Near normal
−1.00 to −1.49	Moderately dry
−1.50 to −1.99	Severely dry
<−2.00	Extremely dry

be expressed in terms of an index, such as the SPI (McKee *et al.*, 1993), used to objectively define drought categories (Table III). McKee *et al.* (1993) suggested fitting the historic rainfall data to a gamma distribution to define SPI, while the Pearson Type 3 distribution has been recommended by Guttman (1999). In this study, the SPI was calculated for each gage using the Gamma distribution for 6-, 12- and 24-month periods. The results

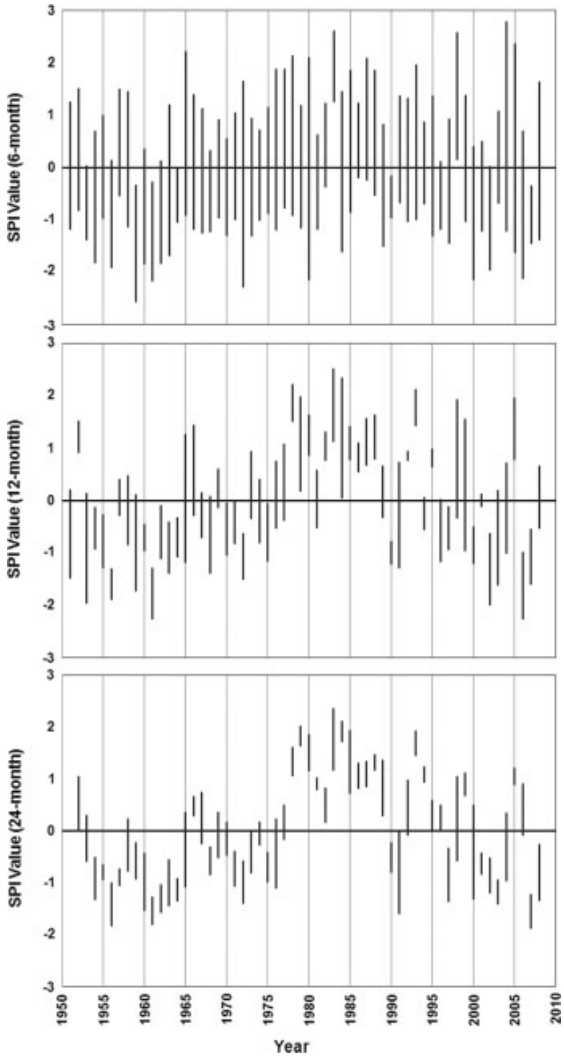

Figure 5. SPI 6-, 12-, and 24-month time scale for climatic Region 1. Each bar shows the range of SPI values over all gages in the region for a given period.

of this analysis are shown in Figure 5, illustrating the high seasonal and interannual variability of precipitation in the region. This analysis also shows considerable spatial variability at the seasonal scale, with stronger spatial consistency in the annual and two-year totals. Perhaps the most evident drought features are in the 24-month time scale. In Region 1, drought episodes occurred in 1954–1965, 1971–1973, and 2000–2004. A similar drought pattern occurred in Region 2.

Although a statistically significant trend was not found in the data, the low SPI values at the end of the record may be associated with an aridity trend projected for the region in the 21st century (e.g. Burke *et al.*, 2006; Seager *et al.*, 2007; Favre and Gershunov, 2008; Milly *et al.*, 2008; Stahle *et al.* (2009). Furthermore, they are consistent with evidence that dry spell length has significantly increased in the southwestern USA (Groisman and Knight, 2008). As explained by Seager *et al.* (2007), decreases in precipitation can be sustained by changes in atmospheric circulation that change the mean moisture convergence at the northern edge of the

subtropics, reducing rainfall in this region. Diffenbaugh *et al*. (2008) found that areas of Northwest Mexico and the Southwest USA are the most susceptible regions to climate change impacts in the 21st century, mainly due to high rainfall variability.

3.3. Annual and seasonal extreme event frequency estimates

Indices such as SPI are useful to define drought categories but do not provide explicit return period estimates. Furthermore, the two-parameter Gamma distribution may not provide reliable frequency estimates for extreme events. Thus, five candidate three-parameter probability distributions were tested to fit the seasonal and annual precipitation data for each region. Table IV shows values of the goodness of fit statistic, Z, for the annual precipitation analysis indicating that the GNO, GEV, and PE3 are acceptable for both regions, meeting the criterion of $|Z| \leq 1.64$. The GLO and GPA distributions were rejected with goodness-of-fit measures of 2.76 and 1.84 for region 1, and −3.86 and −2.88 for region 2, respectively.

Table IV. Goodness-of-fit statistics for acceptable distributions, $|Z^{DIST}| \leq 1.64$, fitted to annual precipitation data.

	Z^{DIST}	
Acceptable distributions	Region 1	Region 2
Generalized normal	0.69	−0.21
Generalized extreme value	0.17	0.16
Pearson Type III	−0.50	−0.98

Table V. Regional quantile estimates of annual precipitation for Regions 1 and 2. Shown are results for 100, 50, 20, 10, and, 5-year return periods, as fraction of the mean, for all acceptable probability distributions. Also shown for comparison are empirical (observed) quantile estimates, based on Hosking and Wallis (1995) plotting positions ($p = (m - 0.35)/n$).

Quantile estimates – Annual – Regional growth curve					
Annual non-exceedance probability	**0.01**	**0.02**	**0.05**	**0.10**	**0.20**
Return period (years)	**100**	**50**	**20**	**10**	**5**
REGION 1					
Gen. normal	0.22	0.26	0.35	0.44	0.57
Gen. extreme value	0.19	0.25	0.34	0.44	0.57
Pearson Type III	0.26	0.29	0.36	0.43	0.56
Observed	0.17	0.22	0.30	0.40	0.56
REGION 2					
Gen. normal	0.21	0.26	0.35	0.44	0.57
Gen. extreme value	0.19	0.25	0.35	0.44	0.58
Pearson Type III	0.25	0.29	0.36	0.44	0.56
Observed	0.13	0.18	0.29	0.41	0.58

Table VI. Regional quantile estimates of two-year precipitation for both regions combined. Results are shown as a fraction of the two-year mean. Also shown for comparison are empirical (observed) quantile estimates, based on Hosking and Wallis (1995) plotting positions ($p = (m - 0.35)/n$).

Quantile estimates – 24 month – Regional growth curve					
Two−year non-exceedance probability	**0.01**	**0.02**	**0.05**	**0.10**	**0.20**
REGIONS 1 & 2					
Generalized pareto	0.18	0.20	0.24	0.31	0.46
Observed	0.16	0.22	0.28	0.38	0.53

Table VII. Regional quantile estimates of seasonal precipitation for Regions 1 and 2. Shown are results for 100, 50, 20, 10, and, 5-year return periods, as a fraction of the mean, for all acceptable probability distributions. The Cold season is from Nov to Apr. Also shown for comparison are empirical (observed) quantile estimates, based on Hosking and Wallis (1995) plotting positions ($p = (m - 0.35)/n$).

Quantile estimates - Cold season – Regional growth curve					
Annual non-exceedance probability	**0.01**	**0.02**	**0.05**	**0.10**	**0.20**
Return period (years)	**100**	**50**	**20**	**10**	**5**
REGION 1					
Pearson Type III	0.23	0.25	0.31	0.38	0.50
Gen. pareto	0.30	0.31	0.34	0.38	0.48
Observed	0.26	0.32	0.35	0.44	0.52
REGION 2					
Pearson Type III	0.19	0.22	0.27	0.34	0.46
Gen. normal	0.13	0.17	0.26	0.35	0.48
Gen. extreme value	0.09	0.15	0.25	0.35	0.49
Observed	0.26	0.29	0.38	0.43	0.50

Tables V, VI and VII show the quantile estimates for the annual, two-year, and cold season (Nov−Apr) periods, respectively, for the acceptable distributions. The quantiles are expressed as percentages of the mean precipitation in the corresponding time period. For instance, for a site in region 1, an annual precipitation total as small as 26% of the mean annual precipitation is estimated to occur on average once in 50 years. It can be observed that for annual rainfall intensities in the range of 5- to 100-year recurrence intervals, the three distributions provide very consistent estimates. For return periods of 100 years and greater, quantiles of the candidate distributions begin to diverge, and comparisons

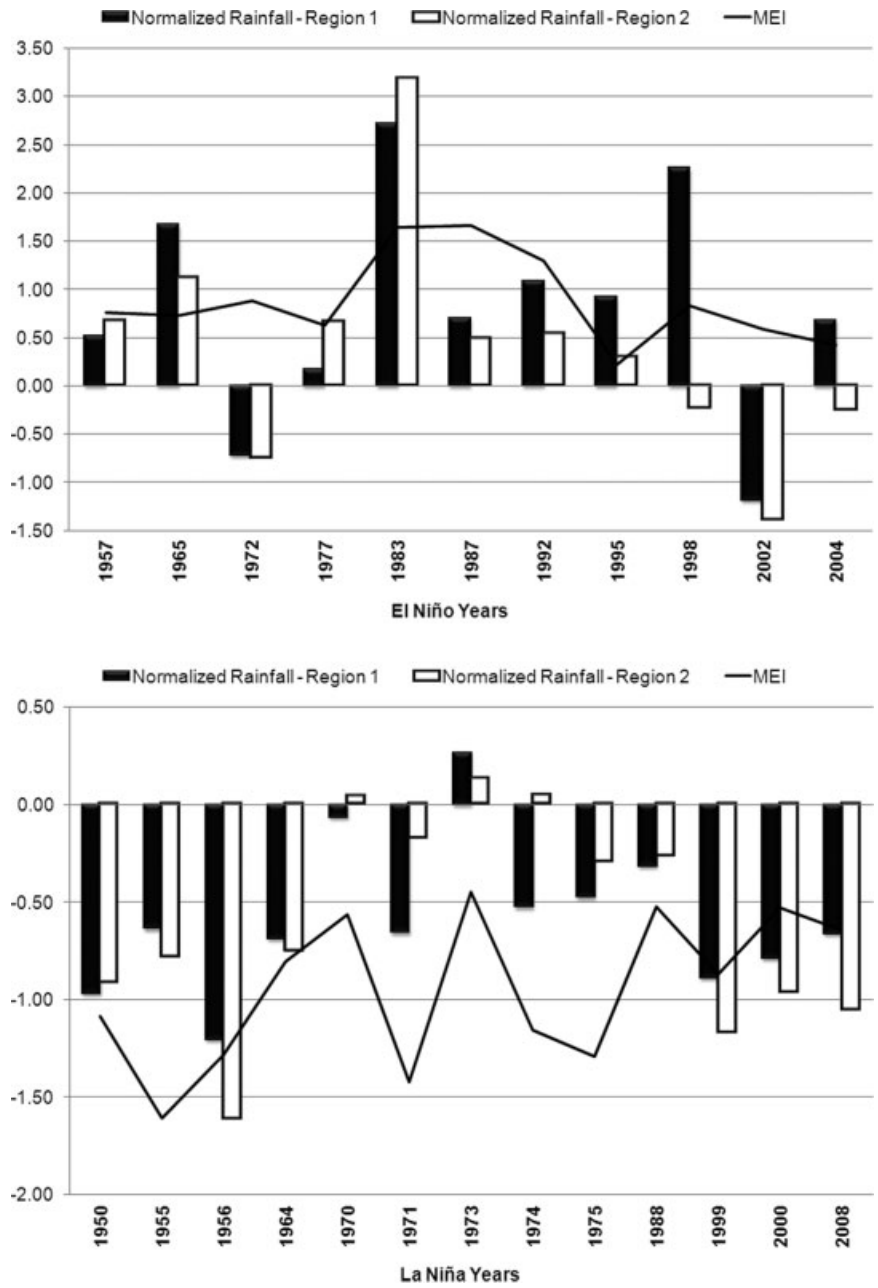

Figure 6. Association of MEI and normalized rainfall for climatic Regions 1 and 2 during El Niño (top) and La Niña (bottom) episodes. Correlation coefficients between annual MEI and normalized rainfall for Regions 1 and 2 are 0.54 and 0.44, respectively.

to the observed data are useful. Considering Region 1, where approximately 1% of the annual precipitation values are less than 1.6 inches (40 mm), which is about 16% of the mean annual precipitation, the GEV quantile estimate of 19% of the mean is closer than those of the other candidate distributions (22 and 26%). Thus, out of the three acceptable candidate distributions, the GEV distribution was the most consistent for the annual time scale in comparisons with empirical estimates for both regions, in addition to having the best goodness of fit statistic (lowest absolute value of Z), given in Table V.

For the two-year analysis, missing data and short record lengths required the two regions to be combined. Only the GPA distribution provided an acceptable fit to the data. As shown in Table VI, quantiles of the regional growth curve are slightly smaller than corresponding annual quantiles, indicating the region is prone to multi-year droughts (also illustrated in Figure 5). Limited data prevented regional frequency analysis for longer durations.

In the seasonal analysis, consistency among acceptable distributions is observed for return periods of 5–20 years for rainfall intensities, similar to the annual analysis. The cold season quantiles are, in fact, comparable to the annual quantiles due to the region following a strong winter precipitation regime. The PE3 distribution is acceptable in both regions, though in Region 1 the GPA distribution is more consistent with the empirical values. More discrepancies between the distribution and

Table VIII. Annual and seasonal correlations between ENSO events and precipitation. Seasonal correlation coefficients are between winter precipitation (Nov–Apr) and winter MEI.

	Region 1	Region 2
Annual		
El NIÑO	0.38	0.54
LA NIÑA	0.48	0.18
NEUTRAL	0.36	0.25
ALL	0.54	0.44
Winter season		
El NIÑO	0.70	0.64
LA NIÑA	0.60	0.65
NEUTRAL	0.36	0.42
ALL	0.59	0.57

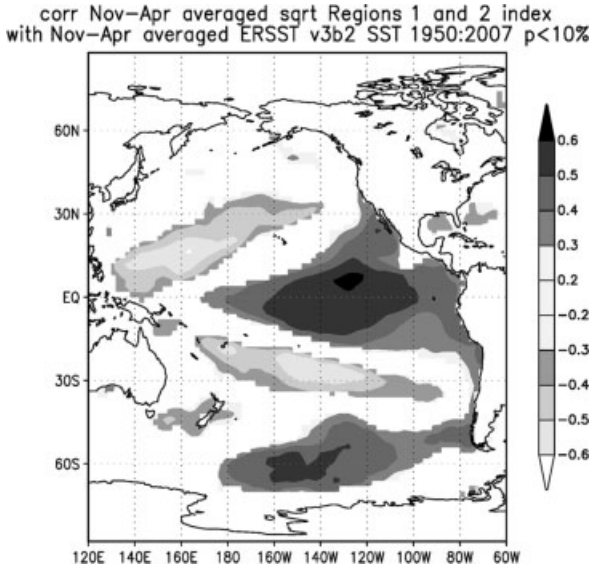

Figure 7. Corelation map of winter (November–April) rainfall in Regions 1 and 2 with winter sea surface temperatures, 1950–2007 ($p < 0.10$).

empirical values are observed in the warm season (not shown), notably for Region 2. This variability is due to a small seasonal dataset (with a significant amount of missing data), as well as very small precipitation values during this season.

3.4. ENSO-conditioned drought frequencies

In this investigation it was demonstrated that a strong ENSO teleconnection with seasonal and annual rainfall in the study region exists, as shown in Figure 6, in which normalized average annual precipitation data and MEI are plotted for El Niño and La Niña years in both precipitation regions. In most years, positive MEI values coincide with above normal rainfall, indicating wet years during El Niño events, and vice versa for La Niña events. Correlation coefficients for annual and seasonal precipitation and MEI are shown in Table VIII. Winter precipitation (Nov–Apr) and winter MEI have the highest correlation coefficients. In addition, correlations between

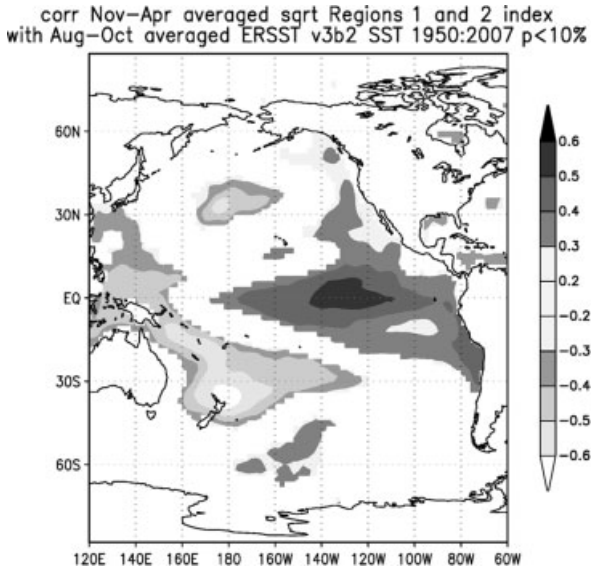

Figure 8. Corelation map of winter (November–April) rainfall in Regions 1 and 2 with preceding summer (August–October) sea surface temperatures, 1950–2007 ($p < 0.10$).

winter-precipitation (Nov–Apr) and winter SST patterns (Figure 7) were investigated, again showing strong correlation with ENSO activity. Since SST patterns are persistent (i.e. have significant autocorrelation), there is also strong correlation between winter precipitation and summer (leading) SSTs, as shown in Figure 8. This indicates the ability to forecast precipitation based on SST persistence.

For the purpose of supporting drought prediction, the regional drought frequency analysis was repeated for three regimes: El Niño, La Niña, and Neutral years (Non-ENSO). Due to missing data, only a single homogeneous climate region was used for this analysis, and the number of stations varied due to missing data for each regime and some discordant sites being removed: the El Niño (EN) analysis included 15 stations; analysis of La Niña (LN) years included 17 stations; and analysis of Neutral (N) years included 28 stations. Also, for the EN region the analysis period was adjusted to 1977–1998 due to years with 6 or less consecutive months of data. The LN and N regions were analysed for the entire period of record (1950–2008). Out of the five candidate distributions, three distributions acceptably fit the three ENSO-conditioned regions, GLO, GNO, and GEV. The quantile estimates for all acceptable distributions are shown in Table IX. Notably, for sites in the EN analysis, the 5-year recurrence interval drought (based on analysis of all years, 57% of the mean, as shown in Table V), has less than a 1% chance of occurring given an EN event. For sites in the LN analysis, the 50-year recurrence interval drought (29% of the mean, as shown in Table V) has a 5% chance of occurring given a LN event.

These results confirm the findings of others (e.g. Cayan *et al.*, 1999; Cavazos and Rivas, 2004; Seager, 2007) and are consistent with the 1997–1998 El Niño-event that produced heavy rainfall in northwest Baja

Table IX. ENSO-conditioned quantile estimates of mean annual precipitation. The probability distributions show results for 100, 50, 20, 10, and, 5-year return periods.

Quantile estimates – Regional growth curve					
Annual non-exceedance probability	**0.01**	**0.02**	**0.05**	**0.10**	**0.20**
Return period (years)	**100**	**50**	**20**	**10**	**5**
El Niño					
Gen. logistic	0.60	0.72	0.91	1.06	1.25
Pearson Type III	0.74	0.80	0.92	1.04	1.21
Gen. normal	0.72	0.79	0.92	1.04	1.23
Gen. extreme value	0.70	0.79	0.92	1.04	1.23
La Niña					
Gen. logistic	0.03	0.15	0.30	0.42	0.54
Pearson Type III	0.10	0.18	0.30	0.40	0.52
Gen. normal	0.10	0.18	0.30	0.40	0.52
Gen. extreme value	0.12	0.20	0.30	0.40	0.52
Neutral					
Gen. logistic	0.19	0.27	0.39	0.52	0.67
Gen. normal	0.28	0.34	0.42	0.51	0.65
Gen. extreme value	0.26	0.31	0.42	0.52	0.66

California (Reyes-Coca and Troncoso-Gaytan 2001) and the 1999 strong La Niña event that produced below-normal precipitation in northwest Mexico and southwest USA (Arriaga-Ramirez and Cavazos, 2010). In addition, almost all of North America suffered a severe drought during the persistent La Niña of 1998–2002; moreover, no North American drought has occurred that was not concurrent with a phase of persistent La Niña (Seager, 2007). The ENSO-conditioned drought frequency analysis results provide predictive tools for forecasting meteorological drought risk (both probability and severity) in the Guadalupe River Basin, potentially mitigating the impacts of drought, as well as the impacts of drier conditions predicted for the 21st century (e.g. Seager *et al*., 2007; Favre and Gershunov, 2008; Milly *et al*., 2008).

4. Summary and conclusions

This study analysed seasonal and annual precipitation data from 34 sites in northwest Baja California. Two homogeneous climatic regions – a coastal region and a mountain region – were identified, consistent with the precipitation regions proposed by Arriaga-Ramirez and Cavazos (2010). SPI values were computed to characterize drought severity for durations of 6 months, 1 year, and 2 years. The calculation of indices such as SPI on a continuous (real-time) basis is recommended to help identify and monitor local meteorological droughts (McPhee *et al*., 2004). Though the SPI was computed using a Gamma distribution, other distributions that fit the data well may be used.

To derive seasonal and annual drought frequency estimates for long recurrence intervals, the regional L-moments algorithm (Hosking and Wallis 1997) was applied. Of the five three-parameter distributions identified as candidates to fit the regional data, the GEV distribution was deemed most appropriate for the annual frequency analysis, while the PE3 and GNO were selected for the cold and warm season frequency analysis, respectively. The return period estimates presented here are based on the most up-to-date rainfall data, and are recommended for use in water resources design and decision making at the local (watershed) scale.

In the study region, ENSO events have received significant attention in recent years because of improved predictability of ENSO and the extent of its impacts (e.g. Cavazos and Rivas, 2004). In this work, correlation of precipitation in the study area with ENSO was confirmed, with both MEI values and ENSO-like Pacific Ocean SST patterns clearly linked to seasonal and annual rainfall variability. These findings provided motivation for an ENSO-conditioned frequency analysis which could form the basis of future work to develop a rainfall drought forecasting system for the region. Such a forecasting system may provide significant benefits for managing water for irrigation and other uses prior to and during drought periods (Leung *et al*., 2003).

While reliable rainfall forecasts with lead times of even one season can have a significant effect on water systems operations (Karamouz and Zahraie, 2004; Sun *et al*., 2006), future work should also focus on analysis of other hydrologic system components contributing to hydrologic, agricultural, and socioeconomic drought (Medellín-Azuara *et al*., 2007). Better understanding of the seasonal and interannual variability of evaporation, surface runoff, soil moisture, and groundwater is needed, along with humans' ability to manage and adapt to this variability. Ultimately, a drought forecasting model and drought management plan may be included in the Guadalupe River Basin Water Management Plan (CONAGUA 2008) to better prepare, adapt, and respond to drought impacts. The SPI and rainfall drought frequency estimates developed in this study may be useful tools to monitor ongoing meteorological droughts and to assess current climatic conditions in the basin. The SPI has been applied in other drought severity studies in the North America monsoonal region (Cañon *et al*., 2007, Hallack-Alegria and Watkins, 2007).

The methods applied in this study are transferable to other locations. Since ENSO has been linked to rainfall variability in many regions (e.g. Nicholson *et al*., 2001; Gershunov and Cayan, 2003; Singhrattna *et al*., 2005), the ENSO-conditioned rainfall drought frequency analysis may serve as a model for other studies. In addition, the L-moment regional frequency analysis technique has been widely used (e.g. Fowler and Kilsby, 2003; Wallis *et al*., 2007; Hallack-Alegria and Watkins, 2007) and

may be particularly valuable in other regions with short precipitation records. The results of this study may also have implications for other areas where rainfall variability has been linked to Pacific Ocean SSTs (e.g. Seager *et al*., 2007; White *et al*., 2008), or areas with monsoonal climates that are showing a tendency toward increasing drought occurrence (e.g. Easterling *et al*., 2000) or are predicted to experience drier conditions in the coming century.

Acknowledgements

This research was supported by the Autonomous University of Baja California (UABC). Data used in this study was provided by the National Commission of Water (CONAGUA) in Baja California, and by the Mexican Institute of Water Technology (IMTA). Valuable comments made by Dr Tereza Cavazos of Centro de Investigacion Cientifica y de Educacion Superior de Ensenada (CICESE), and Dr Abraham R. Martin of Universidad de Sonora (UNISON) are appreciated. Any errors are solely the responsibility of the authors.

References

Arriaga-Ramirez S, Cavazos T. 2010. Regional trends of daily precipitation indices in northwest Mexico and the southwest United States. *Journal of Geophysical Research.* **115**: D14111.

Block P, Rajagopalan B. 2007. Interannual variability and ensemble forecast of the Upper Blue Nile Basin Kiremt season forecast. *Journal of Hydrometeorology* **8**: 327–342.

Burke EJ, Brown SJ, Christidis N. 2006. Modeling the Recent Evolution of Global Drought and Projections for the Twenty-First Century with the Hadley Centre Climate Model. *Journal of Hydrometeorology*. **7**: 1113–1125.

Cayan DR, Dettinger MD, Diaz HF, Graham NW. 1998. Decadal Variability of precipitation over western North America. *Jsournal of Climate*. **11**: 3148–3166.

Cayan DR, Redmond KT, Riddle LG. 1999. ENSO and hydrologic extremes in the western United States. *Journal of Climate*. **12**: 2881–2893.

Cavazos T, Rivas D. 2004. Variability of extreme precipitation events in Tijuana, Mexico. *Climate Research* **25**: 229–243.

Cañon J, Gonzalez J, Valdes J. 2007. Precipitation in the Colorado River Basin and its low frequency associations with PDO and ENSO signals. *Journal of Hydrology*. **333**: 252–264.

Comisión Nacional del Agua. 2004. Estadísticas del agua en México, 2004. www.conagua.gob.mx.

Comisión Nacional del Agua. 2006. Estudio para Actualizar la Disponibilidad Media Anual de las Aguas Nacionales Superficiales en las 85 (ochenta y cinco) Subregiones Hidrológicas de las 7 (siete) Regiones Hidrológicas 1, 2, 3, 4, 5, 6 y 7 de la Península de Baja California, Mediante la Aplicación de la NOM-011-CNA-2000.

Comisión Nacional del Agua. 2007. Programa Nacional Hídrico 2007–2012. www.conagua.gob.mx.

Comisión Nacional del Agua. 2008. Manejo Integrado de las Aguas Subterráneas en los Acuíferos Guadalupe, Ensenada, La Misión y Maneadero, Estado de Baja California.

Cook ER, Seager R, Cane MA, Stable DW. 2007. North American droughts: Reconstructions, causes and consequences. *Earth Science Reviews*. **81**: 93–114.

Dai AG, Trenberth KE, Qian TT. 2004. A global dataset of Palmer Drought Severity Index for 1870–2002: relationship with soil moisture and effects of surface warming. *Journal of Hydrometeorology*. **5**(6): 1117–1130.

Diffenbaugh NS, Giorgi F, Pal JS. 2008. Climate change hotspots in the United States, *Geophysical Research Letters.* **35**: L16709.

Favre A, Gershunov A. 2008. North Pacific Cyclonic and Anticyclonic transients in a global warming context: Possible consequences for western North American daily precipitation and temperature extremes. *Climate Dynamics.* **32**: 969–987.

Fowler HJ, Kilsby CG. 2003. A Regional Frequency Analysis of United Kingdom Extreme Rainfall from 1961 to 2000. *International Journal of Climatology*. **23**: 1313–1334.

Easterling DR, Evans JL, Groisman PYa, Karl TR, Kunkel KE, Ambenje P. 2000. Observed Variability and Trends in Extreme Climate Events: A Brief Review. *Bulletin of the American Meteorological Society*. **81**: 417–425.

Gaeta-Lara A. 2006. Productividad de la vid en función del aprovechamiento del agua subterránea en el Valle de Guadalupe 1994–2004. MPA Thesis. Centro de Investigación Científica y de Educación Superior de Ensenada (CICESE), Ensenada, Mexico, 61 pp.

Gershunov A, Cayan DR, 2003. Heavy Daily Precipitation Frequency over the Contiguous United States: Sources of Climatic Variability and Seasonal Predictability. *Journal of Climate*. **16**: 2752–2765.

Guttman NB. 1994. On the Sensitivity of Sample L Moments to Sample Size. *Journal of Climate* **7**: 1026–1029.

Guttman NB. 1999. Accepting the Standardized Precipitation Index: A calculation Algorithm. *Journal of the American Water Resources Association* **35**: 311–322.

Groisman PY, Knight RW. 2008. Prolonged Dry Episodes over the Conterminous United States: New Tendencies Emerging during the Last 40 Years. *Journal of Climate* **21**: 1850–1862.

Hallack-Alegria M. 2005. Drought Frequency Analysis and Prediction for Sonora, Mexico. M.S. thesis, Dept. of civil and Environmental Engineering, Michigan Technological University, Houghton, MI, 65 pp.

Hallack-Alegria M, Watkins Jr. DW. 2007. Annual and Warm season Drought-Intensity-Duration-Frequency Analysis for Sonora, Mexico. *Journal of Climate.* **20**: 1897–1909.

Higgins RW, Silva VBS, Shi W, Larson J. 2007. Relationships between Climate Variability and Fluctuations in Daily Precipitation over the United States. *Journal of Climate* **20**: 3561–3579.

Held IM, Soden BJ. 2006. Robust responses of the hydrological cycle to global warming. *Journal of Climate*. **19**: 5686–5699.

Hoerling MP, Kumar A, Zhong M. 1997. El Niño, La Niña and the nonlinearity of their teleconnections. *Journal of Climate*. **10**: 1769–1786.

Hoerling MP, Kumar A, Xu T. 2001. Robustness of the nonlinear climate response to ENSO's extreme phases. *Journal of Climate.* **14**: 1277–1293.

Hoerling MP, Kumar A. 2003. The perfect ocean for drought. *Science* **299**: 691–694.

Hosking JRM. 1990. L-moments: Analysis and estimation of distributions using linear combinations of order statistics. *Journal of the Royal Statistical Society,* Series B **52**: 105–124.

Hosking JRM, Wallis JR. 1993. Some statistics useful in regional frequency analysis. *Water Resources Research* **29**: 271–281.

Hosking JRM, Wallis JR. 1997. *Regional Frequency Analysis*. Cambridge University Press. 224 pp.

Karamouz MF, Zahraie B. 2004. Seasonal streamflow forecasting using snow budget and El Niño-Southern Oscillation climate signals: Application to the Salt River Basin in Arizona, *Journal of Hydrologic Engineering* **9**(6): 523–533.

Kunkel KE, Bromirski PD, Brooks HE, Cavazos T, Douglas AV, Easterling DR, Emanuel KA, Groisman PYa, Holland GJ, Knutson TR, Kossin JP, Komar PD, Levinson DH, Smith RL. 2008. Observed Changes in Weather and Climate Extremes in Weather and Climate Extremes in a Changing Climate. Regions of Focus: North America, Hawaii, Caribbean, and U.S. Pacific Islands. Karl YR, Meehl GA, Miller CD, Hassol SJ, Waple AM, Murray WL (eds). A Report by the U.S. Climate Change Science Program and the Subcommittee on Global Change Research, Washington, DC.

Labedzki L. 2007. Estimation of Local Drought Frequency in Central Poland using the Standardized Precipitation Index SPI. *Irrigation and Drainage* **56**: 67–77.

Leung LR, Qian Y, Bian X, Hunt A. 2003. Hydroclimate of the Western United States Based on Observations and Regional Climate Simulation of 1981–2000. Part II: Mesoscale ENSO Anomalies. *Journal of Climate* **16**: 1912–1928.

Lu J, Vecchi G, Reichler T. 2007. Expansion of the Hadley Cell under global warming. *Geophysical Research Letters* **34**: DOI:10.1029/2006GL028443.

Medellin-Azuara J, Mendoza-Espinosa LG, Lund JR, Ramirez-Acosta RJ. 2007. The application of an economic-engineering optimization model for water management in Ensenada, Baja California, Mexico. *Water Science & Technology* **55**(1): 339–347.

McKee TB, Doesken NJ, Kleist J. 1993. The relationship of drought frequency and duration to time scales. Preprints, *Eighth Conference*

on Applied Climatology, Anaheim, CA. American Meteorological Society: 179–184.
McPhee J, Comrie A, Garfio G. 2004. Drought and Climate in Arizona CLIMAS Final Report, The University of Arizona, Tucson, AZ, 24 pp.
Milly PCD, Betancourt J, Falkenmark M, Hirsch RM, Kundzewicz ZW, Lettenmaier DP, Stouffer RJ. 2008. Stationarity is dead: Whither Water Management? *Science* **319**: 573–574.
Minnich RA, Viscaino EF, Dezzani RJ. 2000. The El Niño/Southern Oscillation and precipitation variability in Baja California, Mexico. *Atmosfera* **13**: 1–20.
Nicholson SE. 2001. Climatic and Environmental Change in Africa During the Last Two Centuries. *Climate Research* **17**: 123–144.
Oldenborgh GJV, Burgers G. 2005. Searching for decadal variations in ENSO precipitation teleconnections. *Geophysical Research Letters* **32**(15): L15701. DOI:10.1029/2005GL 023110.
Paulo AA, Ferreira E, Pereira LS. 2005. Stochastic Prediction of SPI Drought Class Transitions. *ICID 21st European Regional Conference*. Frankfurt (Oder) and Slubice, Germany and Poland, 15–19 May 2005.
Reyes-Coca S, Troncoso-Gaytan R. 2001. El Niño Oscilación del Sur y los fenómenos hidrometeorológicos en Baja California: el evento de 1997/98. *Ciencia Pesquera*, **15**: (PA: CEOFA20016).
Reyes S, Troncoso R. 2004. Multidecadal modulation of winter rainfall in northwestern Baja California. *Ciencias Marinas* **30**(1A): 99–108.
Schonher T, Nicholson SE. 1989. The relationship between California rainfall and ENSO events. *Journal of Climate* **2**: 1258–1269.
Seager R. 2007. The turn of the century North American Drought: Global context, dynamics, and past analogs. *Journal of Climate* **20**: 5527–5552.
Seager R, Ting M, Held I, Kushnir Y, Lu J, Vecchi G, Huang H, Harnik N, Leetmaa A, Lau N, Li C, Velez J, Naik J. 2007. Model Projections on an imminent transition to a more arid climate in the southwestern North America. *Science* **316**: 1181–1184.
Seager R, Davis M, Cane M, Naik N, Nakamura J, Li C, Cook E, Stahle DW. 2009. Mexican Drought: an observational modeling and tree ring study of variability and climate change. *Atmosfera* **22**(1): 1–31.
Shin HS, Salas JD. 2000. Regional Drought Analysis based on Neural Networks. *Journal of Hydrologic Engineering* **5**: 145–155.
Singhrattna N, Rajagopalan B, Clark M, Kumar K. 2005. Seasonal Forecasting of Thailand Summer Monsoon Rainfall. *International Journal of Climatology* **25**: 649–664.
Smith TM, Reynolds RW, Peterson TC, Lawrimore J. 2008 Improvements to NOAA's Historical Merged Land-Ocean Surface Temperature Analysis (1880–2006).. *Journal of Climate* **21**: 2283–2296.
Stahle DW, Cook ER, Villanueva-Diaz J, Fye FK, Burnette DJ, Griffin RD, Acuña-Soto R, Seager R, Heim RR Jr. 2009. Early 21st-century drought in Mexico. *Eos Trans. AGU* **90**(11): 89–100.
Sun Y, Solomon S, Dai A, Portmann R. 2006. How often does it rain? *Journal of Climate* **19**: 916–934.
Trefry CM, Watkins Jr DW, Johnson DL. 2005. Regional Rainfall Frequency Analysis for the State of Michigan. *Journal of Hydrologic Engineering* **10**(6): 437–449.
Trenberth KE, Hurrell JW. 1994. Decadal atmosphere-ocean variations in the Pacific. *Climate Dynamics* **9**: 303–319.
Waller-Barrera C. 2008. Optimización del manejo del agua de uso urbano de Ensenada y uso agrícola de Mandadero y Valle de Guadalupe, B.C. M.S. thesis, Dept. of Sciences, Universidad Autonoma de Baja California, BC, Mexico, 103 pp.
Wallis JR, Schaefer MG, Barker BL, Taylor GH. 2007. Regional precipitation-frequency analysis and spatial mapping for 24-hour and 2-hour durations for Washington State. *Journal of Hydrology & Earth System Sciences* **11**(1): 415–442.
Watkins Jr DW, Link GA, Johnson DL. 2005. Mapping Regional Precipitation Intensity-Duration-Frequency Estimates. *Journal of the American Water Resources Association* **41**(1): 157–170.
Wei W, Watkins Jr DW. 2011. Probabilistic Streamflow Forecasts Based on Hydrologic Persistence and Large-Scale Climate Signals in Central Texas. *Journal of Hydroinformatics* (in press). DOI:10.2166/hydro.2010.133.
Wang Z, Chang C-P, Wang B. 2007. Impacts of El Niño and La Niña on the U.S. Climate during Northern Summer. *Journal of Climate* **20**: 2165–2177.
White WB, Gershunov A, Annis J. 2008. Climatic Influences on Midwest Drought during the Twentieth Century. *Journal of Climate* **21**: 517–531.
Wolter K, Timlin MS. 1993. Monitoring ENSO in COADS with a seasonally adjusted principal component index, *Proc. of the 17th Climate Diagnostics Workshop, Norman, OK. NOAA/NMC/CAC, NSSL*, Oklahoma Clim. Survey, CIMMS and the School of Meteor., Univ. of Oklahoma, 52–57.
Wu H, Hayes MJ, Wilhite DA, Svoboda MD. 2005. The effect of the length of record on the standardized precipitation index calculation. *International Journal of Climatology* **25**: 505–520.
Zhu C, Lettenmaier D. 2007. Long-Term Climate and Derived Surface Hydrology and Energy Flux Data for Mexico: 1925–2004. *Journal of Climate* **20**: 1936–1946.

